World Academy of Science, Engineering and Technology
International Journal of Physical and Mathematical Sciences
Vol:6, No:5, 2012

A Novel Single-Wavelength All-Optical Flip-Flop Employing Single SOA-MZI

H. Kaatuzian, M. Sedghi and S. Khatami

***Abstract*—**In this paper, by exploiting a single semiconductor optical amplifier-Mach Zehnder Interferometer (SOA-MZI), an integratable all-optical flip-flop (AOFF) is proposed. It is composed of a SOA-MZI with a bidirectional coupler at the output. Output signals of both bar and crossbar of the SOA-MZI is fed back to SOAs located in the arms of the Mach-Zehnder Interferometer (MZI). The injected photon-rates to the SOAs are modulated by feedback signals in order to form optical flip-flop. According to numerical analysis, Gaussian optical pulses with the energy of 15.2 fJ and 20 ps duration with the full width at half-maximum criterion, can switch the states of the SR-AOFF. Also simulation results show that the SR-AOFF has the contrast ratio of 8.5 dB between two states with the transition time of nearly 20 ps.

***Keywords*—**All Optical, Flip-Flop, Mach-Zehnder Interferometer (MZI), Semiconductor Optical Amplifier (SOA).

I. Introduction

ALL-OPTICAL devices are one of the key components of the next generation optical signal processing systems. As well as needing for high speed optical communication in the current era, all optical signal processing is also critical for future finite state systems. Sequential optical machines, optical data packet switching and routing require all-optical logic gates and flip-flops. Optical time division multiplexed (OTDM) communication systems operating at single wavelength need for kind of flip-flops which work with single wavelength.

Several efforts have been carried out by scientists for implementing all-optical flip-flops (AOFFs). But most of those work with two wavelengths. A large number of AOFFs are based on lasers and bistability in lasing modes. coupled semiconductor micro-ring lasers [1], coupled laser diodes [2], microdisk lasers on silicon chip [3] and multimode interference bistable laser diodes [4] are used for all-optical flip-flop operation in this category. In [5] a new concept for AOFFs was proposed. It is composed of two coupled ring laser at two wavelengths. Each cavity in this configuration has a semiconductor optical amplifier (SOA) as an active element. The same as flip-flop in [5], An AOFF including two unidirectional ring lasers was proposed in [6]. It uses separate cavities and sharing a same active element unidirectionally. Thence, several optical flip-flops [7],[8] were introduced base on the AOFF core in [5]. AOFFs using polarization can be found in [9]. Coupled interferometric switches also can be used for forming AOFFs [10],[11]. In [11] a AOFF was proposed based on two coupled Mach Zehnder Interferometers (MZI) which employs SOA in MZI arms. Some kind of flip-flops based on a single semiconductor optical amplifier- Mach Zehnder Interferometer (SOA-MZI) were introduced in [12],[13].

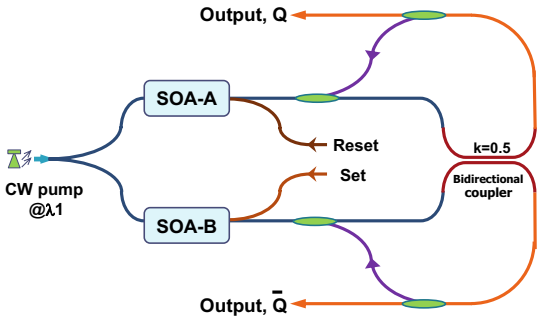


Fig. 1 The proposed set-reset all-optical flip-flop.

In addition to laser based flip-flops, all of the SOA-MZI optical flip-flops work at two wavelengths. It means that wavelengths of optical set-reset inputs and optical outputs are different. So cross gain modulation (XGM) and cross phase modulation (XPM) are nonlinear phenomena's of SOA corresponding for phase shifting in arms of MZI. Operating in two wavelengths leads to inability of cascading sequenced optical flip-flops. Furthermore working with two wavelengths requires wavelength conversion.

In this paper, for the first time to our knowledge, a new architecture for single wavelength set-reset all-optical flip-flop (SR-AOFF) exploiting a single SOA-MZI is proposed. The SR-AOFF is depicted in Fig. 1. Small footprint and single wavelength operation are the considerable features of the SR-AOFF for optical integrated circuits. Using of two SOAs in both arms of MZI and feeding back of both outputs in a differential exciting configuration, lead to increase the switching speed and reduce the minimum energy level of trigger pulses.

The rest of the paper is organized as follows: Section II describes the proposed SR-AOFF qualitatively and discusses its operational principle. Theoretical analysis of the SR-AOFF is explained in section III. In section IV, time domain simulation of the AOFF is carried out. Discussion and conclusion are in section V.

Hassan Kaatuzian is with the Photonics Research Laboratory, Electrical Engineering Department, Amirkabir University of Technology, Tehran, Iran (phone: +982164543388; e-mail: hsnkato@aut.ac.ir).

Mohammad Sedghi is with the Photonics Research Laboratory, Electrical Engineering Department, Amirkabir University of Technology, Tehran, Iran (e-mail: m.sedghi@aut.ac.ir).

Saeid Khatami is with the Semiconductor Devices Research Laboratory, Electrical Engineering Department, Amirkabir University of Technology, Tehran, Iran (e-mail: khatami@aut.ac.ir).

Open Science Index, Physical and Mathematical Sciences Vol:6, No:5, 2012 publications.waset.org/4727/pdf

Open Science Index, Physical and Mathematical Sciences Vol:6, No:5, 2012 publications.waset.org/4727/pdf

II. Operation Principle

The proposed SR-AOFF is shown in Fig. 1. It is composed of one MZI cell containing a SOA in its each arm. The SOA-MZI is fed by a continuous wave (CW) called pump laser. A bidirectional coupler with the coupling factor of 0.5 is placed at the end of the MZI. A bit power of each output of the bidirectional coupler (naming bar and crossbar output ports) is collected to make feedback signals injecting to SOAs located in arms of the MZI. The suggested AOFF has two outputs ($Q,\bar{Q}$) at the same wavelength (λ_1). One output is the inverted version of the other output. The bulk power of outputs of the bidirectional coupler forms the outputs of the SR-AOFF ($Q,\bar{Q}$). In a proper design, just one of the outputs and consequently one of the feedback signals have non-negligible optical power. Variations of feedback signals affect differentially the injected photon rate to SOAs. As shown in Fig. 1, set and reset signals are injected to the SOA-MZI in opposite direction of the CW pump propagation. Both set and reset signals have the same wavelength λ_1.

Since the set, reset, and pump signals have the same wavelength, the gain material of SOA is a function of carrier density [14]. Carrier density is modulated by total photon rates injected to SOA [15]. Optical gain of SOA is decreased if the total photon rate injecting to SOA is increased. This leads to self-gain modulation (SGM) and self-phase modulation (SPM). The AOFF employs a SOA-MZI as an all-optical switch. This switch is controlled by the photon rate injected to the SOAs. Unbalanced photon rate injection into SOAs of each arm causes switching the output power from one port to another. An exact analysis of a SOA-MZI switch is given in section III.

For changing the state of the SR-AOFF, a trigger pulse should be applied to one of the input ports which is corresponding to the zero-level output. The trigger pulse causes gain variation of the encountering SOA. Thus this leads to changing in propagating phase of that arm. According to section III, these changes cause variation of the output powers. In the transition between two states, feedback signals change the photon rate injected to SOAs differentially. Therefore, phase differences in arms of the SOA-MZI will be changed with the value of π Radians occurring in a positive feedback. Afterwards, the outputs will be stable on the other state. In the steady state, the phase difference in arms is $+\pi$ and $-\pi$ for two stable states respectively.

III. Theoretical Analysis

Different subsystems of the proposed SR-AOFF must be inspected in order to analyze the whole structure. SOA-MZI is a nonlinear optical switch that requires time domain analysis by solving the differential wave and rate equations. In this section the SOA model used for the current simulation work is described and the transfer function of a SOA-MZI is extracted and discussed.

A. SOA model

Light amplification occurs in active region which is activated by current injection. Carrier density is changed when light enters the active region due to excitation of electrons in the conductance band [15]. Change in the carrier density causes a change in the material gain. A complex formula for material gain is given in [16]. For single wavelength, the material gain (g_m) can be approximated as follows [14].

$$g_m(z,\tau) = a\left(n(z,\tau) - n_t\right). \tag{1}$$

Where a is differential material gain, $n(z,\tau)$ is carrier density, and n_t is carrier density at transparency.

Using the rate equation for a single optical input for SOA, the rate of carrier density is calculated from (2) as follows [14]:

$$\frac{\partial n(z,\tau)}{\partial \tau} = \frac{I}{qV} - \frac{n(z,\tau)}{\tau_c} - \frac{\Gamma g_m(n)\left|A(z,\tau)\right|^2}{hf.WH}. \tag{2}$$

In (2) A is the intensity of optical electric field. It is a complex scalar responsible for both amplitude and phase of the electric filed. Γ is optical confinement factor, h is Plank's Constant, f is the frequency of injected light, τ_c is carrier life time, q is electric charge, I is injected current, V is volume of active region, and W and H are width and height of active region respectively as shown in Fig. 2.

In (2), diffusion process is neglected. Furthermore, gain dispersion and group velocity have been neglected because their effects are negligible for typical amplifier lengths (L= 0.2mm to 0.5mm) and pulsewidths > ~10 ps [17]. Equation (2) is valid for optical pulses more than 10 ps and CW signals.

It is worth mentioning that SOAs show rich carrier dynamics in terms of processes occurring on different timescales and they are very important in determining the performance of SOA-MZI switch. Among these processes, two photon absorption (TPA), free carrier absorption (FCA) and spectral hole burning (SHB) are almost instantaneous process and for pulses narrower than several picoseconds and subpicoseconds, cannot be ignored [18].

Using Maxwell equations and assuming slow variation along the SOA length and using retarded time frame [17] according to

$$\tau = t - z/v_g, \tag{3}$$

(v_g is group velocity), the intensity of optical electric field is determined as following [14].

$$\frac{\partial A(z,\tau)}{\partial z} = \frac{j\omega_0\Gamma}{2\bar{n}C}\chi A(z,\tau) - \frac{1}{2}\alpha_{int}A(z,\tau). \tag{4}$$

In (4), $\bar{n}$ is the effective mode index, ω_0 is the atomic transition frequency, C is the velocity of light in vacuum, α_{int} is internal loss, and χ is the susceptibility that represents

Open Science Index, Physical and Mathematical Sciences Vol:6, No:5, 2012 publications.waset.org/4727/pdf

the effect of injected carriers on the dielectric constant. According to a phenomenological model, χ is determined as follows [17]:

$$\chi = -\frac{\bar{n}C}{\omega_0}(j+\alpha)g_m(n). \quad (5)$$

In (5) α is the line width enhancement factor. It is the ratio of the change in the real part of the index to its imaginary part. The typical values of α are in the range of 3 to 8 [14].

Equations (2) and (4) are usable only for single optical excitation. If multiple optical signals are injected into the SOA with similar wavelength (i.e. in the case of the proposed AOFF) or with different wavelength, (2) and (4) can be modified as follows:

$$\frac{\partial n(z,\tau)}{\partial \tau} = \frac{I}{qV} - \frac{n(z,\tau)}{\tau_c} - \frac{1}{WH}R_{ph}(z,\tau), \quad (6)$$

$$p_i \frac{\partial A_i(z,\tau)}{\partial z} = \frac{j\omega_0\Gamma_i}{2\bar{n}C}\chi_i A_i(z,\tau) - \frac{1}{2}\alpha_{int}A_i(z,\tau). \quad (7)$$

Where, R_{ph} denotes the total photon rate injecting into a differential element (dz) along z axes (propagating direction). R_{ph} is related to input optical signals by

$$R_{ph}(z,\tau) = \sum_{i=1}^{r}\frac{\Gamma_i g_{mi} A_i(z,\tau)A_i^*(z,\tau)}{hf_i}, \text{ (r: number of inputs)} \quad (8)$$

In (7), p_i determines the propagation direction of each optical signal. Its values are +1 or −1 for propagation in z or – z direction, respectively. By substituting (5) into (7) and neglecting α_{int} and by defining effective net gain as

$$g_i = \Gamma_i g_{mi}, \quad (9)$$

the intensity of the optical electric field is given by

$$p_i \frac{\partial A_i(z,\tau)}{\partial z} = \frac{1}{2}g_i(z,\tau)(1-j\alpha)A_i(z,\tau). \quad (10)$$

Furthermore, by substituting (1) in (6), the effective gain can be calculated as follows:

$$\frac{\partial g_i(z,\tau)}{\partial \tau} = \frac{g_{0,i}-g_i(z,\tau)}{\tau_c} - \frac{a\Gamma_i}{WH}R_{ph}(z,\tau).$$
$$g_{0,i} = a\Gamma_i\left(\frac{I\tau_c}{qV} - n_t\right) \quad (11)$$

Equations (10) and (11) must be solved simultaneously for finite segmentation of SOA along z direction in each finite time frame. A system level analysis with many SOAs requires an extended simulation time. With the help of some useful approximations, (10) and (11) can be approximated for time domain solution. Assuming a constant gain along the length of the SOA and using (10), $R_{ph}^{avg}(\tau)$ the average of $R_{ph}(z,\tau)$ is given by

$$R_{ph}^{avg}(\tau) = \sum_{i=1}^{r}\frac{A_i(0,\tau)A_i^*(0,\tau)}{Lhf_i}\left(\exp(g_i(\tau)L)-1\right). \quad (12)$$

Assuming a constant gain and using of $R_{ph}^{avg}(\tau)$, (10) and (12) are changed to:

$$A_i(L,\tau) = A_i(0,\tau)\exp\left(g_i(\tau)(1-j\alpha)L/2\right), \text{ for } p_i = +1$$
$$A_i(0,\tau) = A_i(L,\tau)\exp\left(-g_i(\tau)(1-j\alpha)L/2\right), \text{ for } p_i = -1 \quad (13)$$

$$\frac{\partial g_i(\tau)}{\partial \tau} = \frac{g_{0,i}-g_i(\tau)}{\tau_c} - \frac{a\Gamma_i}{WH}R_{ph}^{avg}(\tau). \quad (14)$$

This study uses (13) and (14) for simulation of the proposed SR-AOFF.

B. SOA-MZI transfer function

A SOA-MZI is composed of three cascaded blocks: A beam splitter, SOAs in MZI arms, and the bidirectional coupler. Outputs of SOA-MZI are calculated as follows:

$$\begin{pmatrix} A_A \\ A_B \end{pmatrix} = T_{\text{bi-coupler}} \times T_{\text{branches}} \times T_{\text{splitter}} \times A_{\text{pump}}. \quad (15)$$

A_A and A_B are outputs of SOA-MZI, T_x determines the transformation matrix of x, and A_{pump} is the intensity of CW input pump which is a complex scalar. Transformation matrix of the bidirectional coupler, $T_{\text{bi-coupler}}$, is determined as follows [19]:

$$T_{\text{bi-coupler}} = \begin{pmatrix} \sqrt{1-k} & -j\sqrt{k} \\ -j\sqrt{k} & \sqrt{1-k} \end{pmatrix}. \quad (16)$$

In (16), k is the coupling factor with the default value of 0.5. Equivalent transformation matrix of splitter and SOA branches can be calculated by (17):

$$T_{\text{branches}} \times T_{\text{splitter}} = \begin{pmatrix} e^{\left(\frac{g_A(\tau)(1-j\alpha)L}{2}\right)} & 0 \\ 0 & e^{\left(\frac{g_B(\tau)(1-j\alpha)L}{2}\right)} \end{pmatrix}\begin{pmatrix} \frac{1}{\sqrt{N}} \\ \frac{1}{\sqrt{N}} \end{pmatrix}. \quad (17)$$

Subscripts A and B are used to distinguish two branches of MZI. N is the number of split signals (i.e. two in the suggested SR-AOFF). g_A and g_B dynamically change with time. Normalized steady-state characteristic curve of a SOA-MZI is

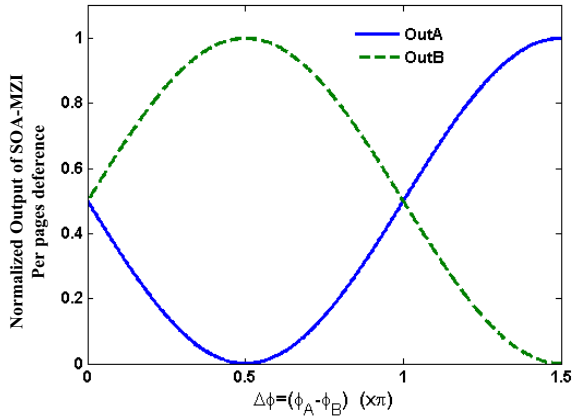


Fig. 2 Normalized steady-state characteristic curve of SOA-MZI.

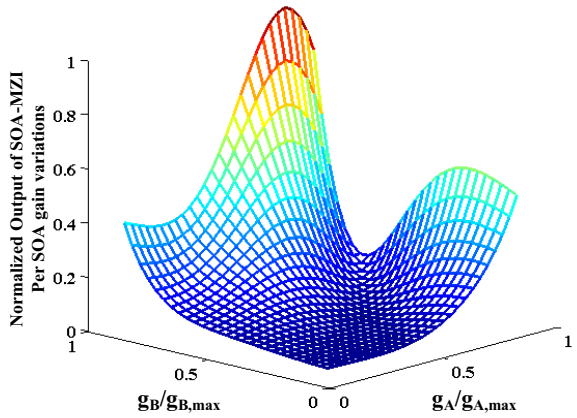


Fig. 3 Normalized Outputs of a typical SOA-MZI switch.

drawn in Fig. 2 as a function of phase difference in the MZI arms. But because of high nonlinearity and gain variation of SOAs in the MZI, the phase differences are varied by the gain variation of SOAs. For a good understanding of how a SOA-MZI switch works, a three-dimensional (3D) graph of one of the SOA-MZI outputs in space of SOA net gain variation, is drawn in Fig. 3. The graph has a peak line and a valley line for specific gain values of SOAs. When the output signals are fed back to the SOAs, two stable states of the SR-AOFF will be created and located in these lines.

From (12) and (14), changes in the input power lead to photon rate ($R_{ph}^{avg}(\tau)$) variations. This causes changes in g_A and g_B. Therefore the optical outgoing power from one output port can be switched to other port. In a good design, the bar and crossbar outputs of SOA-MZI modulate the gain of SOAs making a bistable optical device.

IV. Simulation Results

According to relations obtained for SOA-MZI, the proposed SR-AOFF is simulated in time domain for the physical parameters shown in Table I. Set and reset signals are narrow Gaussian pulses with the peak optical power of one milliWatt. In Fig. 4, Simulation timing diagram of the AOFF is depicted. In Fig. 4 (a), set and reset pulses are shown. Fig. 4 (b) shows

TABLE I
Physical Parameters

Parameters	*Symbol*	*Value*	*Unit*
Control & pump wavelength	λ	1550	nm
Differential gain	a	2.78e-20	m^2
Linewidth enhancement factor	α	2	-
Confinement factor	Γ	0.25	-
Carrier density at transparency	n_t	1.4e24	m^{-3}
Carrier life time	τ_c	70	ps
Injected current	I	500	mA
SOA length	L	200	μm
SOA width	W	1.8	μm
SOA height	H	60	nm
Control pulse width (FWHM[a] for gaussian pulse)	τ_{FWHM}	20	ps
Control pulse peak power	P_{SR}	1	mW
CW Pump signal power	P_{CW}	30.1	μW

[a]Full Width at Half-Maximum

AOFF noninverted and inverted outputs.

As shown in Fig. 4, a true set-reset functionality of the SR-AOFF is verified by simulation. The SR-AOFF has contrast ratio of 8.5 dB between two states. Because of using interferometric switch, the contrast ratio will be increased by increasing the CW pump power. Transition times of rising and falling edges between two states are depicted in Fig. 5. The time in Fig. 5 is expanded for showing more details. As it is indicated in Fig. 5 (a), the rising time is 24.6 ps. Falling time is 15.9 ps according to Fig. 5 (b). Transition times are calculated with the 10 % to 90 % criterion. A reduction in the

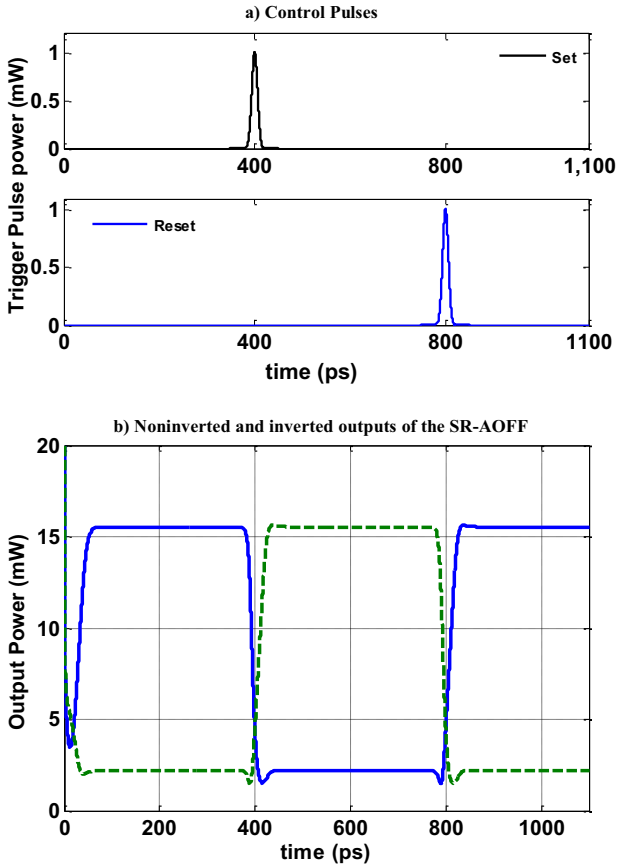


Fig. 4 Time domain simulation of the proposed SR-AOFF,(a) set and reset pulses, (b) noninverting and inverting outputs of the SR-AOFF.

Open Science Index, Physical and Mathematical Sciences Vol:6, No:5, 2012 publications.waset.org/4727/pdf

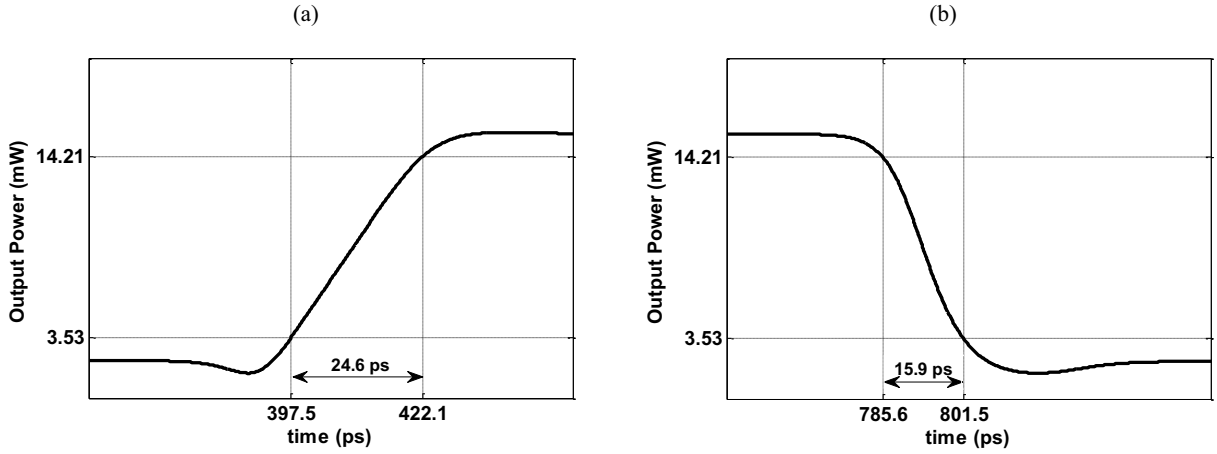


Fig. 5 Transitions between two states, (a) rising time, (b) falling time.

volume of active region leads to an increase the speed. Switching of SR-AOFF can occur with a narrow Gaussian pulse of 20 ps for full width at half-maximum (FWHM) criterion with 15.2 fJ optical energy.

V. Conclusion

A novel set-reset all-optical flip-flop (SR-AOFF) is proposed. Special features of the SR-AOFF are its operation at a single wavelength for both inputs and outputs, small footprint, fast switching and low expiating energy. The time domain simulation of the SR-AOFF verifies correct functionality of a set-reset flip-flop. The simulation results show that excitation pulses with 20 ps duration and optical energy of 15.2 fJ can switch the output states. Setting and resetting transition times are nearly close together and are about 20 ps. The injected current is 500 mA and the output powers of high and low states are about 15.5 milliWatts and 2.2 milliWatts respectively. Physical parameters of SOAs such as confinement factor, differential gain, and linewidth enhancement factor are important for correct flip-flop operation while having less effect on speed. Reducing the volume of the active region and increasing the injection current have more influence on transition time improvements.

References

[1] M. Y. Hill, H. J. S. Dorren, T. de Vries, X. J. M. Leijtens, J. H. den Besten, B. Smalbrugge, Y. S. Oei, H. Binsma, G. D. Khoe, and M. K. Smit, "A fast low-power optical memory based on coupled micro-ring lasers," *Nature,* vol. 432, pp. 206-208, 2004.

[2] M. T. Hil, H. de Waardt, G. D. Khoe, and H. J. S. Dorren, "All-optical flip-flop based on coupled laser diodes," *IEEE Journal of Quantum Electronics,* vol. 37, pp. 405-413, March 2001.

[3] L. Liu, R. Kumar, K. Huybrechts, T. Spuesens, G. Roelkens, E. J. Geluk, T. Vries, P. Regreny, D. V. Thourhout, R. Baets, and G. Morthier, "An ultra-small, low-power, all-optical flip-flop memory on a silicon chip," *Nature Photonics,* vol. 4, pp. 182-187, 2010.

[4] M. Takenaka and Y. Nakano, "Multimode interference bistable laser diode," *IEEE J. of Photonics Technology Letters,* vol. 15, pp. 1035-1037, Aug. 2003.

[5] H. J. S. Dorren, M. T. Hill, Y. Liu, N. Calabretta, A. Srivatsa, F. M. Huijskens, H. D. Waardt, and G. D. Khoe, "Optical packet switching and buffering by using all-optical signal processing methods," *J. Lightw. Technol.,* vol. 21, pp. 2-12, Jan. 2003 2003.

[6] S. Zhang, Y. Liu, D. Lenstra, M. Y. Hill, H. Ju, G. D. Khoe, and H. J. S. Dorren, "Ring-Laser Optical Flip–Flop Memory With Single Active Element," *IEEE J. of Selected Topics in Quantum Electronics,* vol. 10, pp. 1093-1100, 2004.

[7] A. Malacarne, J. Wang, Y. Zhang, A. D. Barman, G. Berrettini, L. Poti, and A. Bogoni, "20 ps Transition Time All-Optical SOA-Based Flip-Flop Used for Photonic 10 Gb/s Switching Operation Without Any Bit Loss," *IEEE Journal of Selected Topics in Quantum Electronics,* vol. 14, pp. 808-815, May-June 2008.

[8] J. Wang, Y. Zhang, A. Malacarne, Y. Minyu, L. Poti, and A. Bogoni, "SOA Fiber Ring Laser-Based Three-State Optical Memory," *IEEE J. of Photonics Technology Letters,* vol. 20, pp. 1697-1699, Oct. 2008.

[9] H. J. S. Dorren, D. Lenstra, Y. Liu, M. Y. Hill, and G. D. Khoe, "Nonlinear Polarization Rotation in Semiconductor Optical Amplifiers: Theory and Application to All-Optical Flip-Flop Memories," *IEEE Journal of Quantum Electronics,* vol. 39, pp. 141-148, 2003.

[10] Y. Liu, R. Mcdougall, M. T. Hill, G. Maxwell, S. Zhang, R. Harmon, F. M. Huijskens, L. Rivers, H. J. S. Dorren, and A. Poustie, "Packaged and hybrid integrated all-optical flip-flop memory " *Electronics Letters* vol. 42, pp. 1399-1400, 2006.

[11] M. Y. Hill, H. D. Waardt, G. D. Khoe, and H. J. S. Dorren, "Fast optical flip-flop by use of Mach–Zehnder interferometers," *Microwave and Optical Technology Letters,* vol. 31, pp. 411-415, 2001.

[12] H. Uenohara, S. Shimizu, T. Kato, Y. Tatara, K. Goto, N. Fukui, and K. Kobayashi, "All-optical flip-flop circuit based on SOA-MZI," in *Communications and Photonics Conference and Exhibition (ACP)*, Asia, 2010, pp. 691-692.

[13] T. Chattopadhyay, C. Reis, P. André, and A. Teixeira, "All-Optical Clocked D Flip-Flop Using a Single SOA-MZI," in *Transparent Optical Networks (ICTON)*, 2011, pp. 1-4.

[14] N. K. Dutta and Q. Wang, *Semiconductor Optical Amplifiers*. Toh Tuck, Singapore: World Scientific Publishing Co. Pte. Ltd., 2006.

[15] H. Kaatuzian, *Photonics* vol. 2. Amirkabir University Press, 2007.

[16] M. J. Connelly, "Wideband semiconductor optical amplifier steady-state numerical model " *IEEE J. Quantum Electron.,* vol. 37, pp. 439-447, 2001.

[17] G. P. Agrawal and N. A. Olsson, "Self-phase modulation and spectral broadening of optical pulses in semiconductor laser amplifiers," *IEEE J. Quantum Electron.,* vol. 25, pp. 2297 - 2306 1989.

[18] J. Mork, J. Mark, and C. Seltzer, "Carrier heating in ingaasp laser ampliers due to two-photon absorption," *Appl. Phys.Lett.,* vol. 64, pp. 2206-2208, 1994.

[19] C. K. Madsen and J. H. Zhao, *Optical Filter Design and Analysis, A Signal Processing Approach*, 1 ed.: Wiley-Interscience, 1999

Open Science Index, Physical and Mathematical Sciences Vol:6, No:5, 2012 publications.waset.org/4727/pdf